Lecture 22, November 4, 2010 (Key Points)

22.1 Parameterization of Basin Response with respect to Drainage Area

Simulated response functions for GCEW change in shape with an increase in spatial scale or drainage area. This change in shape is expressed, on average, by a power law as; see Section 21.3. Although Eq. (21.3) shows that the expected response function changes with *A*, it does not explicitly capture this change-in-shape feature. Therefore, to include this feature, first define $\overline{D}_{2,A} = E[D_{2,A}]$, and define $\bar{f}_{2,A}$ as the normal density function with mean $\overline{\mu}_{2,A}$ and standard deviation $\overline{\sigma}_{2,A}$ that corresponds to $\overline{D}_{2,A}$. Then, from our simulations in Section 21.4, assume that $\overline{\sigma}_{2,A} = \overline{D}_{2,A} = cA^{\lambda}$, where *c* and $0 \le \lambda < 1$ are constants independent of *A*. Accordingly, the expectation of the response function conditioned on $\overline{D}_{2,A}$ is

$$E[W_A(v(t-s)/l)\big|\overline{D}_{2,A}] = (Al/va)\bar{f}_{2,A}(t-s) \tag{22.1}$$

The parameterization with respect to area appears explicitly in Eq. (22.1) via $\overline{\sigma}_{2,A} = cA^{\lambda}$. S'olyom and Tucker (2004) developed a peak flow equation where the time required for water to travel the longest path in a basin is related to *A* via to Hacks Law. Their travel-time relationship is comparable to $\overline{\sigma}_{2,A} = cA^{\lambda}$.

Eq. (22.1) indicates that the basin response function changes non-linearly with spatial scale among subbasins of a basin. This result can be seen explicitly by evaluating the maximum of Eq. (22.1) to get

$$\max_t \mathrm{E}[\mathrm{W_A(vt)}\big|\overline{\mathrm{D}}_{2,\mathrm{A}}] = \frac{lA}{\sqrt{2\pi}va\overline{\sigma}_{2,A}} = \frac{lA^{1-\lambda}}{\sqrt{2\pi}vac} \tag{22.2}$$

This expression shows that the peak of the expected basin response function changes with area as $A^{1-\lambda}$. Veitzer and Gupta (2001) reported a similar empirical relationship between the expected value of the width function peaks and *A*.

22.2 Mean and Maximum Expected discharges

Substituting Eqs. (21.2) and (22.1) into (Lecture 20) gives,

$$\begin{aligned} E[Q_A(t)\big|D_1,\overline{D}_{2,A}] &= (v/l)\int_0^t E[R(s)\big|D_1]E[W_A(v(t-s)/l)\big|\overline{D}_{2,A}]ds; \quad t < T \\ &= E[Z\big|D_1]A\int_0^t f_1(s)f_{2,A}(t-s)ds \end{aligned} \tag{22.3}$$

where f_1 and $\bar{f}_{2,A}$ are Gaussian functions as explained in Lecture 21. Plugging these functions into Eq. (22.3) after algebraic simplifications gives (See, Furey and Gupta (2007) for analytical details not given here),

$$E[Q_A(t)|D_1,\overline{D}_{2,A}] = \frac{E[Z|D_1]A}{\sqrt{2\pi(\sigma_1^2+\overline{\sigma}_{2,A}^2)}}\exp\left(\frac{-(t-\mu_1-\overline{\mu}_{2,A})^2}{2(\sigma_1^2+\overline{\sigma}_{2,A}^2)}\right) \quad (22.4)$$

This equation explicitly shows that the response function of a basin changes in shape with spatial scale because $\overline{\sigma}_{2,A} = cA^{\lambda}$. It can be viewed as a hybrid between a lumped model, because model parameters are spatial-mean values, and a distributed hydrological model because parameters change with respect to spatial scale or drainage area. More complicated models have been formulated that include, for example, a temporally-variable source area for excess rainfall generation and a spatially variable channel-roughness coefficient (Lee and Delleur 1976). However, such models have many parameters and rely on statistical multiple-regression relationships instead of physically based relationships. We have purposefully developed Eq. (22.4) from first principles but included only the most significant physical processes as a first step in applying our diagnostic framework to develop a physical understanding of a complex system (see Lecture 20).

Eq. (22.4) describes the expected discharge from excess rainfall and does not include a base flow component. In river basins like GCEW, base flow is a minor component of streamflow during floods. Consequently, under these conditions the maximum of expected discharge from a single rainfall-runoff (RF-RO) event can be obtained by taking the maximum of Eq. (22.4),

$$Q_m(A) = \max_t E[Q_A(t)|D_1,\overline{D}_{2,A}] = \frac{E[Z|D_1]A}{\sqrt{2\pi(\sigma_1^2+\overline{\sigma}_{2,A}^2)}} \quad (22.5)$$

where the subscript m means maximum and $\overline{\sigma}_{2,A} = cA^{\lambda}$. This equation shows that peak expected discharge depends on the shape of the excess rainfall time series through σ_1^2 and on the shape of the response function through $\overline{\sigma}_{2,A}^2$. It does not depend on the times at which expected excess rainfall and expected basin response peak. Notice that $Q_m(A)$ is the maximum of expected discharge and not the expectation of maximum discharge, that Ogden and Dawdy (2003) reported, for which an analytical expression is quite difficult to obtain.

22.3 Physical Expressions for Scaling Slope and Intercept as Statistical Parameters

First step is to obtain power law parameters from Eq. (22.5) because it is not a power law. Suppose that in log-log space a line connects peak discharge at one scale, *A*, to peak discharge at a larger scale, *bA*, where *b*>1 is a constant. Then, the slope of this line is obtained from,

$$\theta = \frac{\log Q_m(bA) - \log Q_m(A)}{\log bA - \log A} = 1 - \frac{\log\left(\frac{(\sigma_1^2+\overline{\sigma}_{2,A}^2)}{(\sigma_1^2+\overline{\sigma}_{2,bA}^2)}\right)}{\log(1/b)} \quad (22.6)$$

This equation is an approximation for θ obtained from data. It shows that θ is a function of spatial scale because theoretical Eq. (22.5) is not a Power Law as mentioned before. It depends on the time series of excess rainfall through σ_1^2, and on the response functions at scales *A* and *bA* through $\overline{\sigma}_{2,A} = cA^{\lambda}$, and $\overline{\sigma}_{2,bA} = c(bA)^{\lambda}$. Thus, values of θ can change between rainfall events because of changes in σ_1^2 and/or $\overline{\sigma}_{2,A}$ and $\overline{\sigma}_{2,bA}$. The later two terms can change between events because of a change in velocity *v*, as seen by solving for $\overline{\sigma}_{2,bA}$ in Eq. (22.2).

The intercept of the line in log-log space is predicted as,

$$\alpha = \frac{Q_m(A)}{A^{\theta}} == \frac{E[Z|D_1]A^{1-\theta}}{\sqrt{2\pi(\sigma_1^2 + \overline{\sigma}_{2,A}^2)}} \tag{22.7}$$

This equation shows that α can change between rainfall events because of changes in $E[Z|D_1]$, σ_1^2, or in $\overline{\sigma}_{2,A}$ through changes in the velocity *v*. Recall that where, $E[Z|D_1]$ is the expected total depth of excess rainfall given D_1.

When σ_1^2 is fixed, Eq. (22.6) shows that θ is independent of $E[Z|D_1]$ and therefore remains constant as $E[Z|D_1]$ changes. Under the same condition, Eq. (22.7) shows that α changes among events only when $E[Z|D_1]$ changes and it is linearly related to it. These predictions agree with trend 1 reported in Furey and Gupta (2005). When $E[Z|D_1]$ is fixed, the above two equations show that θ and α change non-linearly among events with a change in σ_1^2. Figure 22.1 shows these relationship for $E[Z|D_1]$=1.0, 1.5, and 2.0 cm where $\overline{\sigma}_{2,A} = 50.6A^{0.25}$. Notice that different values of $E[Z|D_1]$ give different curves for α, but the same curve for θ. These predictions agree with trend 2 from Furey and Gupta (2005). Next, the predictions are compared directly with observations.

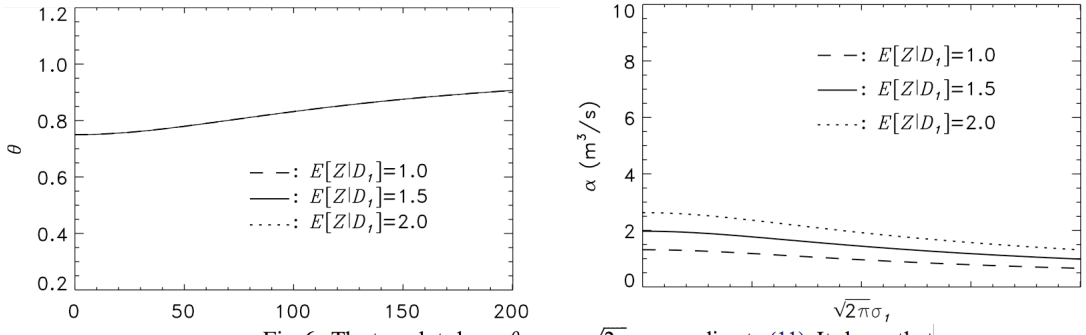

Fig. 6. The top plot shows θ versus $\sqrt{2\pi}\sigma_1$ according to (11). It shows that θ remains the same for different values of $E[Z|D_1]$; observations in [5] for realizations of $Z|D_1$ support this relationship. The bottom plot shows α versus $\sqrt{2\pi}\sigma_1$ according to (12). Here, α represents the peak-discharge that occurs at a drainage area of 1 km^2. Both plots were generated using the simulation result $\bar{\sigma}_{2,A} = 50.6\,A^{0.25}$ ($v_h = 0.1$, $v_l = 1.0$ m/s; see Section 3.3).

Figure 22.1 Changes in Scaling Parameters from Physical Parameters

22.4 Diagnosing Observations in GCEW for a Fixed Value of $E[Z|D_1]$

Values of c and λ in the power law $\overline{\sigma}_{2,A} = cA^{\lambda}$ are needed to diagnose observations using our theoretical predictions. Accordingly, they were obtained from the simulation results where link velocity was fixed to v_l = 1 m/s and hillslope velocity v_h varied among simulations (see Fig. 21.4). The relative influence of v_h on predicted values of θ and α was observed to determine if predictions improve as v_h values reflect more realistic flow conditions. Results from this investigation are discussed below along with the effects of varying link velocity.

Figure 22.2 shows the observed relationships between θ and $\hat{\sigma}$ and predicted mean relationships based on Eq. (22.6). As v_h increases and parameters c and λ change, the predicted relationship between θ and $\hat{\sigma}$ is less consistent with observations. In the case where v_h = ∞, and there are no hillslope effects on streamflow response, the magnitude of θ is under predicted for nearly all events. Thus, a better comparison between theory and observation is obtained when hillslope flow conditions are realistic.

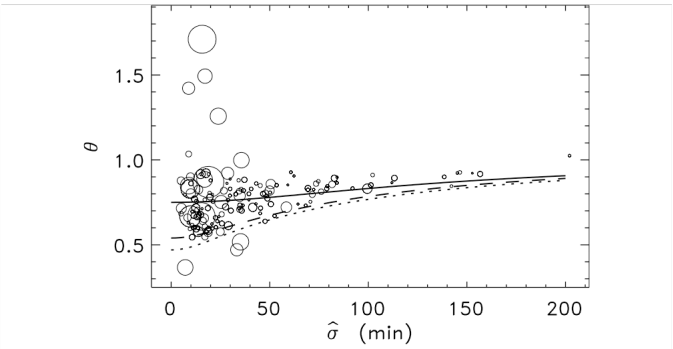

Fig. 7. Exponent θ versus $\hat{\sigma}$ for the 148 events examined in [5]. Each circle denotes an event and circle diameter represents the spatial CV of total rainfall for the event, as determined from the 31 rain gauges in GCEW. As circle diameter increases, so does the spatial variability in total rainfall; see [5]. The three curves are predicted by Eq. (11). For each curve, $b = 21.2/0.172 = 123$ is the ratio of the largest and smallest drainage areas among stream gauges in GCEW. The solid curve is based on the simulation result $\bar{\sigma}_{2,A} = 50.6\,A^{0.25}$ ($v_h = 0.1$, $v_l = 1.0$ m/s), the dashed curve is based on $\bar{\sigma}_{2,A} = 27.05\,A^{0.46}$ ($v_h = 1.0$, $v_l = 1.0$ m/s), and the dotted curve is based on $\bar{\sigma}_{2,A} = 23.51\,A^{0.53}$ ($v_h = \infty$, $v_l = 1.0$ m/s).

Figure 22.2 Observations and predictions of slope with respect to rainfall duration

Figure 22.2 indicates that errors in predicting a mean θ are greatest at low values of $\hat{\sigma}$. Under these conditions, θ depends largely on the value of λ, as shown in Furey and Gupta (2007, Table-1). Therefore, at low values of $\hat{\sigma}$, it is critical to have a good estimate of λ to predict mean θ. This estimate must address both hillslope and network effects on routing water through a basin. If only network effects are addressed, which is the case where v_h = ∞, then λ will be too large to obtain a reasonable prediction. This result suggests that equating response duration to a network-based expression like Hack's Law, as done in SoÅLlyom and Tucker (2004), can lead to significant errors when investigating how peak

streamflows scale with *A* in basins like GCEW. It also complements the finding in D'Odorico and Rigon (2003) that hillslope velocity strongly influences the distribution of residence times of water in basins with relatively small drainage areas.

Figure 22.3 shows observed relationships between α and $\hat{\sigma}$ and predicted mean relationships based on Eq. (22.7). Each plot in the figure represents a narrow range of $\bar{r}_d$ values. Predictions are consistent with observations both with respect to trends and magnitudes. Interestingly, the predictions indicate that the variability in α at a given value of $\hat{\sigma}$ is caused largely by variability in $\bar{r}_d$. This variability decreases as α increases. Also, notice that the middle plot consists of enough points to suggest the presence of a concave relationship between α and $\hat{\sigma}$. This relationship is speculative because of variability among the plotted points. But, it is predicted theoretically, though to a lesser degree than data shows in the middle plot.

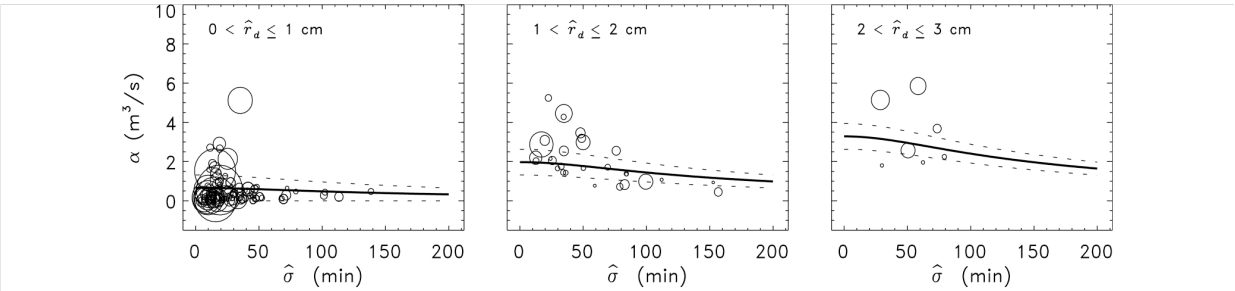

Fig. 8. Coefficient α versus $\hat{\sigma}$ for most of the 148 events examined in [5]; plots are conditioned on a narrow range of $\hat{r}_d$ values and events where $\hat{r}_d > 3$ cm are not shown. As in Fig. 7, circle diameter represents the spatial CV of total rainfall for an event. The curves are predicted by Eq. (12) using the simulation result $\bar{\sigma}_{2,A} = 50.6\,A^{0.25}$ ($v_h = 0.1$, $v_l = 1.0$ m/s). In each plot, the solid curve is for the middle value of $\hat{r}_d$ (e.g. $E[Z|D_1] = \hat{r}_d = 1.5$ in center plot). The dotted curves are for the bounds of $\hat{r}_d$ (e.g. 1 and 2 for lower and upper curves in center plot).

Figure 22.3 Observations and predictions of intercept with respect to rainfall duration

Fury and Gupta (2007) give more detailed discussions of the above results and their limitation. It is recommended to read that paper in detail using Lectures 20, 21 and 22 as a guide.

References

D'Odorico P, and Rigon R. Hillslope and channel contributions to the hydrologic response. *Wat Resour Res.* 2003; 39(5). doi:10.1029/2002WR001708.

Furey, P. R., and V. K. Gupta, Effects of excess rainfall on the temporal variability of observed peak discharge power laws, *Advances in Water Resources* 28, 1240–1253, 2005.

Furey, P. R., and V. K. Gupta, Diagnosing peak-discharge power laws observed in rainfall-runoff events in Goodwin Creek experimental watershed, *Advances in Water Resources*, 30, 2387-2399, 2007

Lee M.T and Delleur J.W. A variable source area model of the rainfall–runoff process based on the watershed stream network. *Water Resour Res.,* 12(5): 1029–36, 1976

Ogden, F. L. and D. R. Dawdy, Peak discharge scaling in a small Hortonian watershed, *Journal of Hydrologic Engineering*, 8(2), 64-73, 2003

SoÅLlyom PB and Tucker GE. Effect of limited storm duration on landscape evolution, drainage basin geometry, and hydrograph shapes. *J Geophys Res.,* 2004;109:F03012. doi:10.1029/2003JF000032.

Veitzer, S., and V. K. Gupta, Statistical self-similarity of width function maxima with implications to floods, *Advances in Water Resources*, 24, 955–965, 2001.